

## CHAPTER 7

---

# ATOMIC MODELS FOR DIFFUSION

---

Macroscopic treatments of diffusion result in continuum equations for the fluxes of particles and the evolution of their concentration fields. The continuum models involve the diffusivity,  $D$ , which is a kinetic factor related to the diffusive motion of the particles. In this chapter, the microscopic physics of this motion is treated and atomistic models are developed. The displacement of a particular particle can be modeled as the result of a series of thermally activated discrete movements (or *jumps*) between neighboring positions of local minimum energy. The rate at which each jump occurs depends on the vibration rate of the particle in its minimum-energy position and the excitation energy required for the jump. The average of such displacements over many particles over a period of time is related to the macroscopic diffusivity. Analyses of *random walks* produce relationships between individual atomic displacements and macroscopic diffusivity.

### 7.1 THERMALLY ACTIVATED ATOMIC JUMPING

The fundamental process in atomistic diffusion models is the thermally activated jump between neighboring sites of local minimum energy. The duration of any jump is typically very short compared to the particle's residence time in a minimum-energy site. Therefore, the average jump rate—the basis for any model of atomistic diffusive motion—is essentially inversely proportional to the average residence time.

The residence time depends upon the probability that the local potential energy will undergo a fluctuation large enough to enable the particle to surmount the

potential-energy barrier that it will encounter while making a jump. This barrier can readily be visualized by considering, as an example, the diffusion of interstitial atoms among the interstices of large substitutional host atoms as described in Section 3.1.4. In this case, a jumping interstitial atom must squeeze its way past the large intervening substitutional atoms to make a successful jump between interstices. This squeezing increases the potential energy in the local region, and a potential-energy barrier to the jump therefore exists. Similar barriers exist for the jumps of particles in other systems. The height of the barrier will depend upon the interaction between the jumping particle and its surroundings and can vary depending upon the path of the jumping particle and the positions of its neighbors. For example, neighboring atoms may cooperatively enlarge the gap through which the jumping particle passes. The complexity of any analysis is increased by this multiplicity of possible activated configurations. However, useful approximations of varying accuracy can be obtained.

There are numerous approaches to modeling the jump rate.<sup>1</sup> Below, three progressively more realistic models are presented. All three approaches produce the same basic result—the jump rate is a product of the vibration frequency in the initial stable site and a Boltzmann probability of a sufficient energy fluctuation for the jump.

### 7.1.1 One-Particle Model with Square Potential-Energy Wells

The simplest model is composed of identical noninteracting particles sitting in rectangular potential-energy wells separated by flat potential-energy barriers. The barriers have widths  $L^A$ , as illustrated in Fig. 7.1. The rate at which the particle traverses a barrier is calculated as a *one-particle event* that occurs in one dimension. The many-bodied aspects are ignored and it is assumed that the migrating particle's surroundings—and therefore the potential-energy landscape—is static. Furthermore, the system is assumed to be in thermal equilibrium, so that the local temperature provides a statistical probability of a particle's kinetic energy fluctuations. Under this condition, a given particle spends most of its time in the energy

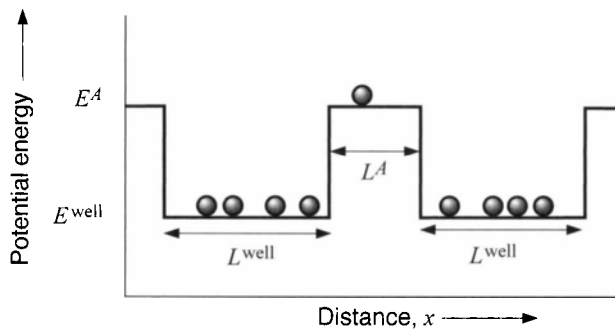


**Figure 7.1:** Square potential-energy wells and an energy barrier for a particle jumping in one dimension. The number of particles is proportional to the occupation probability of well states along  $L^{\text{well}}$  and activated states along  $L^A$ .

<sup>1</sup>See Glasstone et al., Wert and Zener, Vineyard, Rice, Flynn, Girifalco, Christian, and Franklin for examples [1–8].

wells that correspond to low-energy (high-probability) *well states*. However, fluctuations produce brief intervals during which a particle is situated atop the energy barrier along  $L^A$  in high-energy (low-probability) *activated states*. The jump rate is the inverse of the average migration time, the average amount of time between an atom's arrival at one site and its arrival at a neighboring site. The average migration time is the sum of two distinct terms: the time an atom waits to reach an activated state and the migration time in the activated state. It is assumed that the system behaves classically and that any contribution from quantum-mechanical tunneling between the energy wells is negligible. Quantum tunneling can become important for light particles at low temperatures and is discussed elsewhere [5, 8].

The average time for a particle in an activated state to cross the activation barrier is

$$\tau^{\text{cross}} = \frac{L^A}{\langle v \rangle} = L^A \sqrt{\frac{2\pi m}{kT}} \quad (7.1)$$

where  $\langle v \rangle$  is the particle's average velocity along  $L^A$  and  $m$  is its mass. The expression for  $\langle v \rangle$  is found by determining its average momentum  $\langle p \rangle$  and then using  $\langle v \rangle = \langle p \rangle / m$ . In this classical system, the probability that the particle has momentum in the forward direction (i.e., with positive values of  $p$ ) between  $p$  and  $p + dp$  is proportional to  $\exp[-p^2/(2mkT)]dp$  [1]. Therefore,

$$\langle p \rangle = \frac{\int_0^\infty p e^{-p^2/(2mkT)} dp}{\int_{-\infty}^\infty e^{-p^2/(2mkT)} dp} = \sqrt{\frac{mkT}{2\pi}} \quad (7.2)$$

In a system of  $N$  particles, the total rate at which particles cross the barrier,  $\dot{N}^{\text{cross}}$ , is

$$\dot{N}^{\text{cross}} = \frac{\text{number of particles in an activated state}}{\tau^{\text{cross}}} \quad (7.3)$$

Consider a total time  $\tau \gg \tau^A$ , where  $\tau^A$  is the time that a particle spends in an activated state. Then,

$$\dot{N}^{\text{cross}} = \frac{N (\tau^A / \tau^{\text{well}})}{\tau^{\text{cross}}} \quad (7.4)$$

where  $\tau^{\text{well}} \simeq \tau$  is the average duration in a well state. Therefore, for one particle, the crossing frequency (i.e., the *jump frequency*,  $\Gamma'$ ), is

$$\Gamma' = \frac{\tau^A}{\tau^{\text{well}}} \frac{1}{\tau^{\text{cross}}} \quad (7.5)$$

or

$$\Gamma' = \frac{\langle v \rangle}{L^A} \frac{\tau^A}{\tau^{\text{well}}} = \sqrt{\frac{kT}{2\pi m}} \frac{1}{L^A} \frac{\tau^A}{\tau^{\text{well}}} \quad (7.6)$$

The ratio of times spent in a well state and in an activated state is

$$\frac{\tau^A}{\tau^{\text{well}}} = \frac{Z^A}{Z^{\text{well}}} = \frac{\sum_A e^{-E^A/(kT)}}{\sum_{\text{well}} e^{-E^{\text{well}}/(kT)}} \quad (7.7)$$

where  $Z^A$  and  $Z^{\text{well}}$  are the partition functions for the activated and well states.<sup>2</sup>

<sup>2</sup>The partition function plays a central role in statistical mechanics [9]. If the probability of finding a system in a state  $i$  with energy  $E_i$  is proportional to  $\exp[-E_i/(kT)]$ , the partition

If  $\phi(x)$  is the potential energy function illustrated in Fig. 7.1, the classical limit is

$$\frac{\tau^A}{\tau^{\text{well}}} = \frac{\int_{L^A} e^{-\phi(x)/(kT)} dx}{\int_{L^{\text{well}}} e^{-\phi(x)/(kT)} dx} = \frac{L^A}{L^{\text{well}}} e^{-(E^A - E^{\text{well}})/(kT)} \quad (7.8)$$

Therefore,

$$\Gamma' = \sqrt{\frac{kT}{2\pi m}} \frac{1}{L^{\text{well}}} e^{-(E^A - E^{\text{well}})/(kT)} = \left[ \sqrt{\frac{kT}{2\pi m}} \frac{1}{L^{\text{well}}} \right] e^{-E^m/(kT)} \quad (7.9)$$

where  $E^m = E^A - E^{\text{well}}$  (i.e., the height of the barrier) is termed the *activation energy for migration* of the particle. The bracketed term that multiplies the Boltzmann-Arrhenius term  $\exp[-E^m/(kT)]$  has dimensions  $(\text{time})^{-1}$  and represents the number of attempts at the barrier per unit time—the average attempt frequency. The Boltzmann-Arrhenius exponential term is the activation success probability for each attempt. As demonstrated in less simple models below, this simple result—that there is a characteristic attempt frequency multiplied by a Boltzmann-Arrhenius factor containing the activation energy—is quite robust.

### 7.1.2 One-Particle Model with Parabolic Potential-Energy Wells

An improved approximation to the potential-energy landscape can be obtained by introducing parabolic wells and a smooth barrier as in Fig. 7.2.<sup>3</sup> This model is more realistic, as particles that are displaced small distances from their average positions of minimum energy in a solid will generally experience restoring forces that increase linearly with the displacements. This leads to a potential energy that increases as the square of the particle displacement, which corresponds to a static (i.e., non-many-bodied) harmonic model for a solid [9]. The energies of the states of the particles are approximately

$$E(x) = E^{\text{min}} + \frac{\beta}{2} (x - x^{\text{min}})^2 \quad (7.10)$$

In Fig. 7.2, the well states are located in the region denoted by  $L^{\text{well}}$  near the minima. The particles spend the remainder of their time at the approximately flat region denoted by  $L^A$ , where the changes in average particle velocity are small. Particles at other positions experience significant forces from  $-\nabla\phi(x)$  and therefore tend to accelerate, resulting in low occupation probabilities for those positions. The analysis method is the same as that for the rectangular-well model, and Eqs. 7.6 and 7.7 again hold. Using the harmonic potential, the ratio of partition functions

function is related to the normalization factor for the probabilities  $Z = \sum_{\text{states } i} \exp[-E_i/(kT)] = \sum_{\text{energies } j} \Omega(E_j) \exp[-E_j/(kT)] = \sum_{\text{energies } j} \exp(S_j/k) \exp[-E_j/(kT)]$ , where  $\Omega(E_j)$  is the number of states of identical energy  $E_j$ . Because  $Z_A$  is proportional to a sum of probabilities, it is proportional to the total probability of finding a particle in the activated state and therefore the average time in that state.

<sup>3</sup>By illustrating the potential-energy landscape in one dimension in Fig. 7.2, it appears that the activated state is one of maximum energy. The single dimension represents the most likely trajectory between the minimum states which requires the least energy, so the activation energy is that of the trajectory's saddle point—the minimum of all the maximum energies of the trajectories between two minima (see Fig. 7.3).

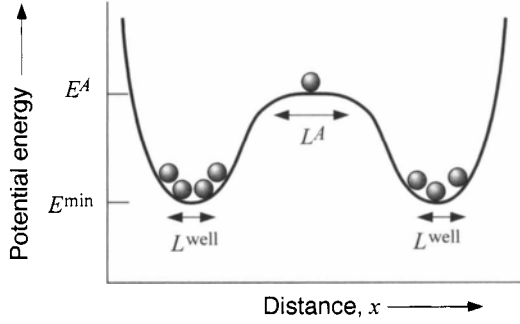


**Figure 7.2:** Parabolic potential-energy well for one-dimensional particle jumps. Unlike the square potential energy function in Fig. 7.1, the energy barrier is no longer perfectly flat.

(Eqs. 7.6 and 7.7) becomes

$$\frac{Z^A}{Z_{\text{well}}} = \frac{\int_{L^A} e^{-E(x)/(kT)} dx}{e^{-E^{\text{min}}/(kT)}} \int_{-L^{\text{well}}/2}^{L^{\text{well}}/2} e^{-[\beta(x-x^{\text{min}})^2]/(2kT)} dx \quad (7.11)$$

and because states far from the well minimum do not contribute significantly, the limits of integration can be approximated with

$$\int_{-L^{\text{well}}/2}^{L^{\text{well}}/2} e^{-[\beta(x-x^{\text{min}})^2]/(2kT)} dx \approx \int_{-\infty}^{\infty} e^{-[\beta(x-x^{\text{min}})^2]/(2kT)} dx \quad (7.12)$$

and integrated to give

$$\Gamma' = \frac{1}{2\pi} \sqrt{\frac{\beta}{m}} e^{-(E^A - E^{\text{min}})/(kT)} = \nu e^{-E^m/(kT)} \quad (7.13)$$

where

$$\nu = \frac{1}{2\pi} \sqrt{\frac{\beta}{m}} \quad (7.14)$$

is the characteristic attempt frequency. Again, the activation energy is the height of the energy barrier and the jump rate is given by an attempt frequency multiplied by a Boltzmann–Arrhenius factor of the form  $\exp[-E^m/(kT)]$ . The frequency,  $\nu$ , is that of a simple harmonic oscillator of mass,  $m$ , with a restoring-force constant given by  $\beta$  (demonstrated in Exercise 7.1).

### 7.1.3 Many-Body Model

The two simple single-body models can be improved by including many-body aspects and by allowing the jumping particle to differ from the remaining particles. A treatment similar to Vineyard's is developed [3]. The  $N$ -body system consists of  $N - 1$  identical particles of mass  $m$  and a single migrating particle of mass  $m_J$ . The state of such a system of  $N$  interacting particles can be defined by  $3N$  spatial coordinates,  $q_i$ , and  $3N$  momenta,  $p_i$ , and can then be represented by a point in a  $6N$ -dimensional phase space with coordinates  $(q_1, q_2, \dots, q_{3N}, p_1, p_2, \dots, p_{3N})$  [9]. Furthermore, the total energy of such a system can be expressed as the sum of its

kinetic energy (a function of the  $3N$  momenta) and its potential energy (a function of the  $3N$  spatial coordinates).

Assuming that there are numerous sites in the system that the jumping particle can occupy while maintaining a stable system structure, the rate at which this particle jumps from one stable site to another can be determined. Figure 7.3a depicts how the total potential energy of the system,  $\phi = \phi(q_1, q_2, \dots, q_{3N})$ , varies as the jumping particle occupies positions throughout the system, including the sites of local minimum energy. Because it is impossible to make such a plot in three dimensions, the many displacements of particles in the system that accompany the displacement of the jumping particle are suggested by the added multiple axes. Point  $P$  represents the situation of the jumping particle in a stable site while point  $Q$  represents the corresponding situation when the jumping particle is in a neighboring stable site. In both cases, the system is stable because it is at a local potential-energy minimum, as indicated by the two minima in the hypersurface shown in the  $3N$ -dimensional space of Fig. 7.3. In Fig. 7.3b, hypersurfaces of constant potential energy are a function of the  $3N$  coordinates indicated in Fig. 7.3a. [These hypersurfaces are of dimensionality  $3N - 1$  because they are defined by the level sets of  $\phi = \phi(q_1, q_2, \dots, q_{3N})$ , so that  $3N - 1$  coordinates are independent.] There are many choices for a particle trajectory between  $P$  and  $Q$ , but the trajectories that cross the saddle point (located at the point  $P^A$ ) require the smallest energy fluctuation and are the most probable. Therefore, the saddle point energies in the potential-energy landscape determine the transition probabilities. The saddles are present because each minimum is surrounded by neighboring maxima. Neighboring minima pairs have at least one connecting path that has an associated saddle energy; the path between  $P$  and  $Q$  in Fig. 7.3 passes through the saddle point  $P^A$ . The force on a particle exactly at  $P^A$  is zero, but the configuration is an unstable equilibrium. A unique hypersurface,  $S^A$ , passes through  $P^A$  and is

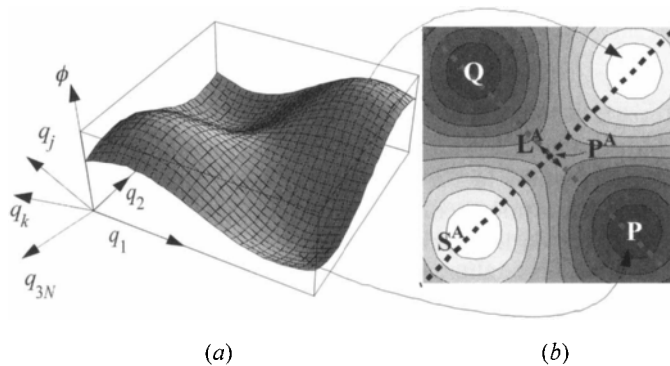


**Figure 7.3:** In a system with  $3N$  spatial coordinates, the potential-energy landscape consists of minima for each of the stable atomic sites, such as  $P$  and  $Q$ . The potential-energy landscape surface (**a** is the surface and **b** shows its isopotentials) represents such a landscape, but only for two spatial coordinates. The surface is impossible to illustrate as a function of all coordinates  $q_1, q_2, \dots, q_{3N}$ . The migrating atom traverses the region between  $P$  and  $Q$  via the saddle point  $P^A$ . During migration the landscape changes in response to the geometrical configuration of the activated state.

perpendicular to the contours of constant  $\phi$ .  $S^A$  constitutes an energy ridge and is analogous to a “continental divide” separating the region associated with  $P$  from the region associated with  $Q$ .

In an equilibrium system, a migrating particle spends most of its time vibrating with small amplitude about low-energy states such as  $P$  and  $Q$ . The crossing time is very short compared to the equilibrium duration, but as the migrating atom crosses, it slows near the saddle point. For the crossing interval depicted in Fig. 7.3, most of the active migration time is spent near saddle points such as  $P^A$  in a volume of the hyperspace centered on the saddle point of width  $L^A$ . Considering the states in the activated volume and the states near the minima, Eqs. 7.6 and 7.7 can be applied to model the jump rate,  $\Gamma'$ , but the analysis must be modified if the system is at constant pressure instead of constant volume. The jump rate for a system at constant temperature and pressure is

$$\begin{aligned}
 \Gamma' &= \sqrt{\frac{kT}{2\pi m_J}} \frac{1}{L^A} \frac{Z_P^A}{Z_P^{\text{well}}} \\
 &= \sqrt{\frac{kT}{2\pi m_J}} \frac{1}{L^A} \frac{e^{-G^A/(kT)}}{e^{-G^{\text{well}}/(kT)}} \\
 &= \sqrt{\frac{kT}{2\pi m_J}} \frac{1}{L^A} \frac{e^{-F^A/(kT)}}{e^{-F^{\text{well}}/(kT)}} \frac{e^{-PV^A/(kT)}}{e^{-PV^{\text{well}}/(kT)}} \\
 &= \sqrt{\frac{kT}{2\pi m_J}} \frac{e^{-P(V^A - V^{\text{well}})/(kT)}}{L^A} \frac{Z^A}{Z^{\text{well}}} \\
 &= \sqrt{\frac{kT}{2\pi m_J}} \frac{e^{-P(V^A - V^{\text{well}})/(kT)}}{L^A} \frac{\sum_{i=1}^N e^{-U_i^A/(kT)}}{\sum_{i=1}^N e^{-U_i^{\text{well}}/(kT)}}
 \end{aligned} \tag{7.15}$$

where  $Z_P$  is the fixed-pressure partition function,  $Z$  is the fixed-volume partition function, and  $V^A$  and  $V^{\text{well}}$  are the system volumes in the activated and well states.

Using  $U_i = p_i^2/2m_i + \phi_i(x)$  in the classical limit [the number of energetically degenerate states =  $(dp dq)/h$ ] and integrating the momentum terms for  $Z$  yields

$$Z = \left( \frac{2\pi m k T}{h^2} \right)^{\frac{3(N-1)}{2}} \left( \frac{2\pi m_J k T}{h^2} \right)^{\frac{3}{2}} \int e^{-\phi(q_1, q_2, \dots, q_{3N})/(kT)} dq_1 dq_2 \cdots dq_{3N} \tag{7.16}$$

To find an expression for the potential energy of the vibrating system in the well state at  $P$ , the harmonic approximation is used and  $\phi(\vec{q})$  is expanded about  $P$ , so the potential-energy surface near  $P$  has the form

$$\phi^{\text{well}}(q_1, q_2, \dots, q_{3N}) = N\phi^\circ + \frac{1}{2} \sum_{i=1}^{3N} \sum_{j=1}^{3N} \left( \frac{\partial^2 \phi}{\partial q_i \partial q_j} \right) \Big|_{q_i=q_i^\circ} (q_i - q_i^\circ)(q_j - q_j^\circ) \tag{7.17}$$

where  $i$  and  $j$  sum over the  $3N$  displacements of the  $J$  atom and the  $N - 1$  other atoms,  $q_i^\circ$  is the average coordinate of the  $i$ th vibrating atom, and  $\phi^\circ$  is the potential energy per atom when all atoms are located in their average positions. The elements of the matrix of second derivatives are the linearized spring constants for each atom site pair and correspond to the quantity  $\beta$  in Eq. 7.10, which was employed in the static harmonic model. Typically, only the near neighbors have nonnegligible entries, the number of which depends on the interatomic potential

length scale. The matrix of second derivatives is real and symmetric and therefore has real eigenvalues, all of which are positive in the stable state. If the  $\delta q_i$  are transformed to its diagonalized coordinate eigensystem  $\delta \eta_i$ ,

$$\phi^{\text{well}}(\eta_1, \eta_2, \dots, \eta_{3N}) = N\phi^\circ + \frac{1}{2} \sum_{i=1}^{3N} m_i \omega_i^2 (\delta \eta_i)^2 \quad (7.18)$$

where  $m_i$  and  $\omega_i$  are the effective masses and characteristic angular frequencies of the three vibrational modes of each harmonic mode and  $i$  now runs over the  $3N$  modes of the  $J$  atom and the  $N - 1$  other atoms. The modes are decoupled in the eigensystem and this transformation exists for any interatomic potential. If the interactions are short-range, the matrix will be sparse and the effective masses and characteristic frequencies will be nearly the same in the eigensystem ( $\eta_i$ ) and the lattice system ( $q_i$ ).

In Eq. 7.16,  $\phi$  can be approximated using Eq. 7.18; the integral's value is dominated by  $\delta \eta_i \approx 0$ , and therefore its limits can be taken to be  $\pm\infty$ , even though the parabolic approximation is valid only near equilibrium,

$$\begin{aligned} & \int e^{-\phi(q_1, q_2, \dots, q_{3N})/(kT)} dq_1 dq_2 \dots dq_{3N} \\ & \approx e^{-N\phi^\circ/(kT)} \left( \int_{-\infty}^{\infty} e^{-m_1 \omega_1^2 \delta \eta_1^2 / (2kT)} d\delta \eta_1 \right) \left( \int_{-\infty}^{\infty} e^{-m_2 \omega_2^2 \delta \eta_2^2 / (2kT)} d\delta \eta_2 \right) \\ & \quad \dots \left( \int_{-\infty}^{\infty} e^{-m_{3N} \omega_{3N}^2 \delta \eta_{3N}^2 / (2kT)} d\delta \eta_{3N} \right) \\ & = e^{-N\phi^\circ/(kT)} \sqrt{\frac{2\pi kT}{m_1 \omega_1^2}} \sqrt{\frac{2\pi kT}{m_2 \omega_2^2}} \dots \sqrt{\frac{2\pi kT}{m_{3N} \omega_{3N}^2}} \\ & = e^{-N\phi^\circ/(kT)} \left( \frac{2\pi kT}{m_J \omega_J^2} \right)^{\frac{3}{2}} \left( \frac{2\pi kT}{m \omega^2} \right)^{\frac{3(N-1)}{2}} \end{aligned} \quad (7.19)$$

where  $\omega$  is the same for all masses except the migrating atom. If the masses and characteristic frequencies differ, a product would appear above for each unique effective mass and characteristic frequency.

When the jumping atom is located along  $L^A$ , where the potential-energy hypersurface has principal curvatures of opposite sign, there is one negative eigenvalue corresponding to the unstable direction along the path between  $P$  and  $Q$  and

$$\begin{aligned} \phi^A & = \sum_i^N \phi_i^A + \frac{1}{2} \left( \frac{\partial^2 \phi^A}{\partial \eta_{J1}^A} \right) \Big|_{\eta_{J1}^A=0} \\ & + \frac{1}{2} m_J (\omega_{J2}^A)^2 (\delta \eta_{J2}^A)^2 + \frac{1}{2} m_J (\omega_{J3}^A)^2 (\delta \eta_{J3}^A)^2 + \frac{1}{2} \sum_{j=1}^{3N-3} m_j (\omega_j^A)^2 (\delta \eta_j^A)^2 \end{aligned} \quad (7.20)$$

where  $i$  iterates over all  $N$  atoms and  $j$  iterates over all but the  $J$  atom.

It is reasonable to assume that only a relatively small number of atoms surrounding the jumping atom are affected when the system goes from the well state to the activated state. Let this number be  $N^A$ . Also, approximate the potential

energy of the jumping atom along  $L^A$  at the saddle point by a parabola in a single variable,  $\eta_{J1}$ . Let the approximating parabola have its maximum  $\phi_J^A$  at  $\delta\eta_{J1} = 0$  and decrease by a factor  $1 - \epsilon$  at  $\delta\eta_{J1} = \pm L^A/2$ :

$$\begin{aligned} \phi^A = & \left[ \phi_J^A + \sum_{i=1}^{N^A} \phi_i^A + (N - N^A - 1)\phi^\circ \right] - \frac{4\epsilon}{(L^A)^2} \phi_J^A (\delta\eta_{J1}^A)^2 \\ & + \frac{1}{2} m_J (\omega_{J2}^A)^2 (\delta\eta_{J2}^A)^2 + \frac{1}{2} m_J (\omega_{J3}^A)^2 (\delta\eta_{J3}^A)^2 \\ & + \frac{1}{2} \sum_{j=1}^{3N^A} m (\omega_j^A)^2 (\delta\eta_j^A)^2 + \frac{1}{2} m \omega^2 \sum_{k=1}^{3(N-N^A-1)} (\delta\eta_k)^2 \end{aligned} \quad (7.21)$$

where  $i$  iterates over all  $N^A$  affected atoms,  $j$  iterates over the  $3N^A$  modes of the affected atoms, and  $k$  iterates over all modes of the  $(N - N^A - 1)$  nonaffected atoms. Equation 7.21 can be integrated with the same approximation employed to obtain Eq. 7.19. To lowest order in  $L^A$  and  $\epsilon$ ,

$$\begin{aligned} & \int e^{-\phi^A/(kT)} d\eta_{J1}^A d\eta_{J2}^A d\eta_{J3}^A d\eta_1^A d\eta_2^A \cdots d\eta_{3N^A}^A d\eta_1 d\eta_1 \cdots d\eta_{3(N-N^A-1)} \\ & = L^A e^{-[\phi_J^A + \sum_{i=1}^{N^A} \phi_i^A + (N - N^A - 1)\phi^\circ]/(kT)} \\ & \times \left[ \frac{2\pi kT}{m_J (\omega_J^A)^2} \right] \left[ \frac{2\pi kT}{m \omega^2} \right]^{\frac{3(N-N^A-1)}{2}} \left( \prod_{\ell=1}^{3N^A} \sqrt{\frac{2\pi kT}{m (\omega_\ell^A)^2}} \right) \end{aligned} \quad (7.22)$$

where  $i$  iterates over all  $N^A$  affected atoms and  $\ell$  iterates over the modes of the affected atoms and it is assumed that  $\omega_{J2}^A = \omega_{J3}^A$ . Therefore,

$$\frac{Z^A}{Z^{\text{well}}} = L^A e^{-[\phi_J^A + \sum_{i=1}^{N^A} \phi_i^A + (N - N^A - 1)\phi^\circ]/(kT)} e^{-N\phi^\circ/(kT)} \frac{\frac{2\pi kT}{m_J (\omega_J^A)^2}}{\left[ \frac{2\pi kT}{m_J (\omega_J^A)^2} \right]^{3/2}} \left( \prod_{\ell=1}^{3N^A} \frac{\omega}{\omega_\ell^A} \right) \quad (7.23)$$

and

$$\Gamma' = \frac{\omega_J}{2\pi} e^{-[\phi_J^A + \sum_{i=1}^{N^A} \phi_i^A - (N^A + 1)\phi^\circ + P(V^A - V^{\text{well}})]/(kT)} \left( \frac{\omega_J}{\omega_J^A} \right)^2 \left( \prod_{\ell=1}^{3N^A} \frac{\omega}{\omega_\ell^A} \right) \quad (7.24)$$

The final expression for the jump rate is then

$$\Gamma' = \nu e^{-G^m/(kT)} = \nu e^{S^m/k} e^{-H^m/(kT)} = \nu e^{-PV^m/(kT)} e^{S^m/k} e^{-U^m/(kT)} \quad (7.25)$$

where

$$\begin{aligned} \nu & = \frac{\omega_J}{2\pi} \\ U^m & = \phi_J^A - \phi^\circ + \sum_{i=1}^{N^A} (\phi_i^A - \phi^\circ) \\ V^m & = V^A - V \\ S^m & = k \left[ 2 \ln \frac{\omega_J}{\omega_J^A} + \sum_{\ell=1}^{3N^A} \ln \left( \frac{\omega}{\omega_\ell^A} \right) \right] \approx \frac{2k(\omega_J^A - \omega_J)}{\omega_J} + \frac{3kN^A \langle \Delta\omega \rangle}{\omega} \end{aligned} \quad (7.26)$$



This sum consists of  $N_\tau \times N_\tau$  products that can be collected into diagonal  $\vec{r}_i \cdot \vec{r}_i$  and off-diagonal ( $\vec{r}_i \cdot \vec{r}_j = \vec{r}_j \cdot \vec{r}_i$ ) parts,

$$\begin{aligned} R^2(N_\tau) &= \sum_{i=1}^{N_\tau} \vec{r}_i \cdot \vec{r}_i + 2 \sum_{j=1}^{N_\tau-1} \sum_{i=j+1}^{N_\tau} \vec{r}_i \cdot \vec{r}_j \\ &= \sum_{i=1}^{N_\tau} |\vec{r}_i|^2 + 2 \sum_{j=1}^{N_\tau-1} \sum_{i=1}^{N_\tau-j} \vec{r}_i \cdot \vec{r}_{i+j} \end{aligned} \quad (7.29)$$

The  $\vec{r}_i \cdot \vec{r}_{i+j}$  can be expressed as products of the jump distances and the cosine of the angle between the jump-vector directions,  $\theta_{i,i+j}$  (i.e.,  $\vec{r}_i \cdot \vec{r}_{i+j} = |\vec{r}_i| |\vec{r}_{i+j}| \cos \theta_{i,i+j}$ ). The mean-square jump distance is

$$\langle r^2 \rangle = \frac{1}{N_\tau} \sum_{i=1}^{N_\tau} |\vec{r}_i|^2 \quad (7.30)$$

Averaging over a large number of independent walkers or trials for a single walker,

$$\langle R^2(N_\tau) \rangle = N_\tau \langle r^2 \rangle + 2 \left\langle \sum_{j=1}^{N_\tau-1} \sum_{i=1}^{N_\tau-j} |\vec{r}_i| |\vec{r}_{i+j}| \cos \theta_{i,i+j} \right\rangle \quad (7.31)$$

Equation 7.31 is general. No assumptions have been made about the randomness of the displacements, the lengths of the various displacements, the allowed values of  $\theta_{i,i+j}$ , or the number of dimensions in which the random walk is occurring.

### 7.2.1 Relation of Diffusivity to the Mean-Square Particle Displacement

A relationship between the macroscopic diffusivity,  $D$ , of a component  $i$  and the mean-square displacement,  $\langle R^2(N_\tau) \rangle$ , can be obtained from the behavior of  $c_i(x, t)$  as it evolves from an initial point source at the origin. Using the solution for diffusion from an instantaneous point source in three dimensions in Table 5.1, the distribution of particles after a time  $\tau$  will be given by

$$c(r, \tau) = \frac{n_d}{(4\pi D\tau)^{3/2}} e^{-r^2/(4D\tau)} \quad (7.32)$$

The second moment of the distribution in Eq. 7.32,

$$\langle R^2(\tau) \rangle = \frac{\int_0^\infty r^2 c(r, \tau) 4\pi r^2 dr}{\int_0^\infty c(r, \tau) 4\pi r^2 dr} \quad (7.33)$$

gives the mean-square displacement away from the original point source. Using Eq. 7.32 and the relationship

$$\int_0^\infty x^4 e^{-ax^2} dx = \frac{3}{8a^2} \sqrt{\frac{\pi}{a}} \quad (7.34)$$

in Eq. 7.33, the mean-square displacement for isotropic three-dimensional diffusion is related to the diffusivity by

$$\langle R^2(\tau) \rangle = 6D\tau \quad (7.35)$$

For diffusion in one and two dimensions, similar calculations show that  $\langle R^2(\tau) \rangle = 2D\tau$  and  $4D\tau$ , respectively. An analogous expression for  $\langle R^2(\tau) \rangle$  when the diffusivity is anisotropic is explored in Exercise 7.4.

Equation 7.35 is a fundamental relationship between the diffusivity and the mean-square displacement of a particle diffusing for a time  $\tau$ . Because diffusion processes in condensed matter are comprised of a sequence of jumps, the mean-square displacement in Eq. 7.31 should be equivalent to Eq. 7.35. This equivalence, as demonstrated below, results in relations between macroscopic and microscopic diffusion parameters.

## 7.2.2 Diffusion and Random Walks

If a particle moves by a series of displacements, each of which is independent of the one preceding it, the particle moves by a *random walk*. Random walks can involve displacements of fixed or varying length and direction. The theory of random walks provides distributions of the positions assumed by particles; such distributions can be compared directly to those predicted to result from macroscopic diffusion. Furthermore, the results from random walks provide a basis for understanding non-random diffusive processes.

The distribution of positions is easily formulated for a random walker on a one-dimensional lattice and illustrates important aspects of all random walks. Such a distribution can be compared to the solution for macroscopic diffusion in Table 5.1. Extensions to two and three dimensions are not difficult. The particles are assumed to migrate independently. A given particle starts at the origin and jumps either forward (along  $+x$ ) with probability  $p_R$  or backward (along  $-x$ ) with probability  $p_L$ , where  $0 < p_R < 1$  and  $p_L + p_R = 1$ . Suppose that each displacement is of length one, then after  $N_\tau \gg 1$  displacements it is possible that the particle will end up at  $-N_\tau, -N_\tau + 1, \dots, -1, 0, 1, \dots, N_\tau - 1, N_\tau$ . It is highly unlikely that the particle will make all positive jumps to reach site  $N_\tau$  or all negative jumps to reach  $-N_\tau$ . If  $p_R = p_L = 1/2$ , then, on average, the particle will be located at the origin because the equally probable positive and negative displacements negate each other. To find the probability that a particle occupies a position  $n$  after  $N_\tau$  jumps, let  $N_R$  be the number of positive displacements and  $N_L$  be the number of negative displacements,

$$N_R - N_L = n \quad (7.36)$$

$$N_R + N_L = N_\tau \quad (7.37)$$

The number,  $\Omega(n, N_\tau)$ , of different ways (trajectories, sequences, etc.) the walker can get to site  $n$  from the origin is given by the binomial coefficient

$$\Omega(n, N_\tau) = \frac{N_\tau!}{N_R! N_L!} = \frac{N_\tau!}{[(N_\tau + n)/2]! [(N_\tau - n)/2]!} \quad (7.38)$$

Therefore, the probability of getting to site  $n$  after  $N_\tau$  jumps is

$$p(n, N_\tau) = \frac{N_\tau!}{[(N_\tau + n)/2]! [(N_\tau - n)/2]!} p_R^{N_R} p_L^{N_L} \quad (7.39)$$

If the probability of jumping right,  $p_R$ , is equal to the probability of jumping left,  $p_L$ ,

$$p(n, N_\tau) = \frac{N_\tau!}{[(N_\tau + n)/2]! [(N_\tau - n)/2]!} \left(\frac{1}{2}\right)^{N_\tau} \quad (7.40)$$

Using Stirling's formula,

$$Q! = \sqrt{2\pi Q} Q^Q e^{-Q} \quad (7.41)$$

and taking the limit  $n/N_\tau \ll 1$  yields

$$p(n, N_\tau) \propto e^{-n^2/(2N_\tau)} \quad (7.42)$$

Equation 7.42 shows that the distribution of a point source in one dimension spreads as a Gaussian.

Letting  $R = n\langle r^2 \rangle^{1/2}$ , the probability distribution for the displacement  $R$  is

$$p(R, N_\tau) \propto e^{-R^2/(2\langle r^2 \rangle \Gamma \tau)} \quad (7.43)$$

The probability distribution must be normalized, so that

$$\int_{-\infty}^{\infty} p(R, \tau) dR = 1 \quad (7.44)$$

Therefore, the probability distribution becomes

$$p(R, N_\tau) = \frac{1}{\sqrt{2\pi N_\tau \langle r^2 \rangle}} e^{-R^2/(2\langle r^2 \rangle \Gamma \tau)} \quad (7.45)$$

which is of the same form as the macroscopic solution for one-dimensional diffusion from a point source in Table 5.1.

The first and second moments of Eq. 7.45 are readily evaluated:

$$\langle R \rangle = \int_{-\infty}^{\infty} p(R, N_\tau) R dR = 0 \quad (7.46)$$

and

$$\langle R^2 \rangle = \int_{-\infty}^{\infty} p(R, N_\tau) R^2 dR = N_\tau \langle r^2 \rangle \quad (7.47)$$

Equation 7.46 demonstrates that if each jump of a walk occurs randomly (i.e., is uncorrelated), the average displacement is zero and the center of mass of a large number of individual random jumpers is not displaced. Equation 7.47 gives the mean-square displacement of a random walk,  $N_\tau \langle r^2 \rangle$ . Although Eqs. 7.46 and 7.47 were derived here for one-dimensional random walks, both are valid for two- and three-dimensional random walks.

The probability distribution of a random walk shows that the mean-square displacement after  $N_\tau$  jumps is  $\langle R^2 \rangle = N_\tau \langle r^2 \rangle = \Gamma \tau \langle r^2 \rangle$  (Eq. 7.47). Comparison of the probability distribution (Eq. 7.45) to the point-source solution for one-dimensional diffusion from a point source (Table 5.1) indicates that

$$D = \frac{\Gamma \langle r^2 \rangle}{2} \quad (7.48)$$

Equation 7.48 relates the macroscopic diffusivity and microscopic jump parameters for uncorrelated diffusion in one dimension.

### 7.2.3 Diffusion with Correlated Jumps

The calculated root-mean-square displacement for a general sequence of jumps has two terms in Eq. 7.31. The first term,  $N_\tau \langle r^2 \rangle$ , corresponds to an ideal random walk (see Eq. 7.47) and the second term arises from possible correlation effects when successive jumps do not occur completely at random.

For walks with correlations,<sup>5</sup> a *correlation factor*,  $\mathbf{f}$ , can be defined

$$\mathbf{f} = 1 + \frac{2}{N_\tau \langle r^2 \rangle} \left\langle \sum_{j=1}^{N_\tau-1} \sum_{i=1}^{N_\tau-j} |\vec{r}_i| |\vec{r}_{i+j}| \cos \theta_{i,i+j} \right\rangle \quad (7.49)$$

so that Eq. 7.31 becomes

$$\langle R^2 \rangle = N_\tau \langle r^2 \rangle \mathbf{f} \quad (7.50)$$

For a random walk,  $\mathbf{f} = 1$  because the double sum in Eq. 7.49 is zero and Eq. 7.50 reduces to the form of Eq. 7.47. In principle,  $\mathbf{f}$  can have a wide range of values corresponding to physical processes relating to specific diffusion mechanisms. This is readily apparent in extreme cases of perfectly correlated one-dimensional diffusion on a lattice via nearest-neighbor jumps. When each jump is identical to its predecessor, Eq. 7.49 shows that the correlation factor  $\mathbf{f}$  equals  $N_\tau$ .<sup>6</sup> Another extreme is the case of  $\mathbf{f} = 0$ , which occurs if each individual jump is exactly opposite the previous jump. However, there are many real diffusion processes that are nearly ideal random walks and have values of  $\mathbf{f} \approx 1$ , which are described in more detail in Chapter 8.

The relationship between the macroscopic isotropic diffusivity,  $D$ , and microscopic jump processes can be evaluated in three dimensions. The equivalence of Eqs. 7.31 and 7.35 means that

$$\langle R^2(N_\tau) \rangle = N_\tau \langle r^2 \rangle + 2 \left\langle \sum_{j=1}^{N_\tau-1} \sum_{i=1}^{N_\tau-j} |\vec{r}_i| |\vec{r}_{i+j}| \cos \theta_{i,i+j} \right\rangle = 6D\tau \quad (7.51)$$

Substitution of Eq. 7.49 into Eq. 7.51 yields the relation between the macroscopic isotropic diffusivity and microscopic parameters

$$D = \frac{\langle r^2 \rangle N_\tau \mathbf{f}}{6\tau} = \frac{\Gamma_\tau \langle r^2 \rangle}{6\tau} \mathbf{f} = \frac{\Gamma \langle r^2 \rangle}{6} \mathbf{f} \quad (7.52)$$

Equation 7.52 is of central importance for atomistic models for the macroscopic diffusivity in three dimensions (see Chapter 8). For isotropic diffusion in a system of dimensionality,  $d$ , the generalized form of Eq. 7.52 is

$$D = \frac{\Gamma \langle r^2 \rangle}{2d} \mathbf{f} \quad (7.53)$$

Equations 7.52 and 7.53 reduce to  $D$  for random-walking particles (i.e., Eq. 7.48) where there are no correlations and  $\mathbf{f} = 1$ .

Values of  $\mathbf{f}$  for several diffusion mechanisms are discussed in Section 8.2.1.

<sup>5</sup>Correlated jumps are discussed in Chapter 8.

<sup>6</sup>There are  $(N_\tau^2 - N_\tau)/2$  cosine terms in the double sum and all are equal to unity.

**Bibliography**

1. S. Glasstone, K.J. Laidler, and H. Eyring. *The Theory of Rate Processes*. McGraw-Hill, New York, 1941.
2. C.A. Wert and C. Zener. Interstitial atom diffusion coefficients. *Phys. Rev.*, 76(8):1169–1175, 1949.
3. G.H. Vineyard. Frequency factors and isotope effects in solid state rate processes. *J. Chem. Phys. Solids*, 3(1–2):121–127, 1957.
4. S.A. Rice. Dynamical theory of diffusion in crystals. *Phys. Rev.*, 112(3):804–811, 1958.
5. C.P. Flynn. *Point Defects and Diffusion*. Oxford University Press, Oxford, 1972.
6. L.A. Girifalco. *Statistical Physics of Materials*. John Wiley & Sons, New York, 1973.
7. J.W. Christian. *The Theory of Transformations in Metals and Alloys*. Pergamon Press, Oxford, 1975.
8. W.M. Franklin. Classical and quantum theory of diffusion in solids. In A.S. Nowick and J.J. Burton, editors, *Diffusion in Solids, Recent Developments*, pages 1–72. Academic Press, New York, 1975.
9. D.A. McQuarrie. *Statistical Mechanics*. HarperCollins, New York, 1976.

**EXERCISES**

- 7.1** Prove that the pre-exponential frequency factor given by Eq. 7.14 is indeed the frequency of a linear oscillator of mass,  $m$ , and force constant,  $\beta$ .

**Solution.** The equation of motion of a linear oscillator is

$$F(x) = -\beta x(t) = m \frac{d^2 x}{dt^2} \quad (7.54)$$

where  $x(t)$  is the displacement of the mass from the position where the restoring force,  $F$ , is zero. The solution of Eq. 7.54 is of the form  $x(t) = A \sin(\omega t)$  where  $A = \text{constant}$ . Substitution of  $x(t)$  in Eq. 7.54 shows that

$$\omega = 2\pi\nu = \sqrt{\frac{\beta}{m}} \quad (7.55)$$

- 7.2** The quantity  $V^m$ , given by Eq. 7.26, is the difference between the volume of the system in an activated state and a well state. This volume difference is generally termed the *activation volume* for migration and is a positive quantity because of the atomic squeezing and resulting expansion of the system that occurs in the activated state. The activation volume can be measured experimentally by measuring the pressure dependence of the jump frequency,  $\Gamma'$ . Find an expression for the pressure dependence of  $\Gamma'$  and describe how it can be used to determine  $V^m$ .

**Solution.** Use Eq. 7.25 for  $\Gamma'$  and differentiate  $\Gamma'$  with respect to pressure, so that

$$\left[ \frac{\partial \ln \Gamma'}{\partial P} \right]_T = \left[ \frac{\partial \ln \nu}{\partial P} \right]_T - \frac{1}{kT} \left[ \frac{\partial G^m}{\partial P} \right]_T \quad (7.56)$$

Using the standard thermodynamic relation  $[\partial G/\partial P]_T = V$  and realizing that the pressure dependence of  $\ln \nu$  will be relatively very small, we may write to a good approximation

$$\left[ \frac{\partial \ln \Gamma'}{\partial P} \right]_T \cong -\frac{1}{kT} V^m \quad (7.57)$$

If a plot of  $\ln \Gamma'$  vs.  $P$  is now constructed using the experimental data,  $V^m$  can be determined from its slope.

**7.3** Consider small interstitial atoms jumping by the interstitial mechanism in b.c.c. Fe with the diffusivity  $D$  for a time  $\tau$ .

- (a) What is the most likely expected total displacement after a large number of diffusional jumps?
- (b) What is the standard deviation of the total displacement?

*Solution.*

- (a) The expected total displacement will be zero because there is no correlation between successive jumps—after a jump the interstitial loses its memory of its jump and makes its next jump randomly into any one of its nearest-neighbor sites.
- (b) The distribution of displacements will be Gaussian (Eq. 7.32) and the standard deviation will be the root-mean-square displacement given by Eq. 7.35 as  $\sqrt{6D\tau}$ .

**7.4** Suppose the random walking of a diffusant in a primitive orthorhombic crystal where the particle makes  $N_1$  jumps of length  $a_1$  along the  $x_1$  axis,  $N_2$  jumps of length  $a_2$  along the  $x_2$  axis, and  $N_3$  jumps of length  $a_3$  along the  $x_3$  axis. The three axes are orthogonal and aligned along the crystal axes of the orthorhombic unit cell and the diffusivity tensor in this axis system is

$$D = \begin{bmatrix} D_{11} & 0 & 0 \\ 0 & D_{22} & 0 \\ 0 & 0 & D_{33} \end{bmatrix} \quad (7.58)$$

- (a) Find an expression for the mean-square displacement in terms of the numbers of jumps and jump distances.
- (b) Find another expression for the mean-square displacement in terms of the three diffusivities in the diffusivity tensor and the diffusion time. Your answer should be analogous to Eq. 7.35, which holds for the isotropic case.

*Solution.*

- (a) Using Eqs. 7.30 and 7.31,

$$\langle R^2 \rangle = \sum_{i=1}^N \vec{r}_i \cdot \vec{r}_i = N_1 a_1^2 + N_2 a_2^2 + N_3 a_3^2 \quad (7.59)$$

- (b) The diffusion equation will have the form of Eq. 4.61. By using the method of scaling described in Section 4.5 (based on the scaling relationships in Eq. 4.64), the solution can be written

$$c(x_1, x_2, x_3, t) = \frac{A}{\sqrt{t}} \exp \left[ - \left( \frac{x_1^2}{4D_{11}t} + \frac{x_2^2}{4D_{22}t} + \frac{x_3^2}{4D_{33}t} \right) \right] \quad (7.60)$$

where  $A = \text{constant}$ . The mean-square displacement is then

$$\begin{aligned} \langle R^2 \rangle &= \frac{\int_0^\infty \int_0^\infty \int_0^\infty c(x_1, x_2, x_3, t) r^2 dx_1 dx_2 dx_3}{\int_0^\infty \int_0^\infty \int_0^\infty c(x_1, x_2, x_3, t) dx_1 dx_2 dx_3} \\ &= \frac{\int_0^\infty \int_0^\infty \int_0^\infty e^{-\frac{x_1^2}{4D_{11}t}} e^{-\frac{x_2^2}{4D_{22}t}} e^{-\frac{x_3^2}{4D_{33}t}} (x_1^2 + x_2^2 + x_3^2) dx_1 dx_2 dx_3}{\int_0^\infty \int_0^\infty \int_0^\infty c(x_1, x_2, x_3, t) dx_1 dx_2 dx_3} \end{aligned} \quad (7.61)$$

Equation 7.61 can be factored into standard definite integrals and the result is

$$\langle R^2 \rangle = 2D_{11}t + 2D_{22}t + 2D_{33}t \quad (7.62)$$

Comparison of Eqs. 7.59 and 7.62 shows that the mean-square displacement consists of three terms, each of which is the mean-square displacement that would be achieved in one dimension along one of the three coordinate directions.

- 7.5** Suppose a random walk occurs on a primitive cubic lattice and successive jumps are uncorrelated. Show explicitly that  $\mathbf{f} = 1$  in Eq. 7.49. Base your argument on a detailed consideration of the values that the  $\cos \theta_{i,i+j}$  terms assume.

*Solution.* Because all jumps are of the same length,

$$\begin{aligned} \mathbf{f} &= 1 + \frac{2}{N_\tau} \sum_{j=1}^{N_\tau} \sum_{i=1}^{N_\tau-j} \langle \cos \theta_{i,i+j} \rangle \\ &= 1 + \frac{2}{N_\tau} \langle \cos \theta_{1,2} + \cos \theta_{1,3} \cdots + \cos \theta_{2,3} + \cos \theta_{2,4} \cdots + \cos \theta_{N_\tau-1, N_\tau} \rangle \end{aligned} \quad (7.63)$$

and thus,

$$\mathbf{f} = 1 + \frac{2}{N_\tau} [\langle \cos \theta_{1,2} \rangle + \langle \cos \theta_{1,3} \rangle + \cdots + \langle \cos \theta_{2,3} \rangle \cdots + \langle \cos \theta_{N_\tau-1, N_\tau} \rangle] \quad (7.64)$$

Any jump can be one of the six vectors:  $[a00]$ ,  $[\bar{a}00]$ ,  $[0a0]$ ,  $[0\bar{a}0]$ ,  $[00a]$ , and  $[00\bar{a}]$ . Each occurs with equal probability. For each pair of jump vectors,  $i$  and  $i+j$ , the six possible values of  $\cos \theta_{i,i+j}$  are 1,  $-1$ , 0, 0, 0, and 0, and these occur with equal probability. For a large number of trajectories, each mean value in Eq. 7.64 is zero and therefore  $\mathbf{f} = 1$ .

- 7.6** For the diffusion of vacancies on a face-centered cubic (f.c.c.) lattice with lattice constant  $a$ , let the probability of first- and second-nearest-neighbor jumps be  $p$  and  $1-p$ , respectively. At what value of  $p$  will the contributions to diffusion of first- and second-nearest-neighbor jumps be the same?

*Solution.* There is no correlation and, using Eq. 7.29,

$$\langle R^2 \rangle = N_\tau \langle r^2 \rangle = \sum_{i=1}^{N_\tau} \bar{r}_i \cdot \bar{r}_i \quad (7.65)$$

The number of first nearest-neighbor jumps is  $N_\tau p$  and the number of second nearest-neighbor jumps is  $N_\tau(1-p)$ . Therefore,

$$\langle R^2 \rangle = N_\tau p \frac{a^2}{2} + N_\tau(1-p)a^2 \quad (7.66)$$

They make equal contributions when  $N_\tau p a^2 / 2 = N_\tau(1-p)a^2$  or  $p = 2/3$ .